

# Accurate representation of formation energies of crystalline alloys with many components

A. Shapeev

*Skolkovo Institute of Science and Technology, Skolkovo Innovation Center, Nobel Str. 3, Moscow 143026, Russia*

(Dated: May 23, 2022)

In this Letter I propose a new model for representing the formation energies of multicomponent crystalline alloys as a function of atom types. While the state-of-the-art cluster expansion method so far could only be applied to, at most, quaternary systems, I demonstrate the application of the proposed method to a septenary system over the entire range of its compositions. The proposed model has only two tunable parameters—one for the interaction range and one for the interaction complexity.

Accurate computational prediction of properties of alloys from their composition is one of the outstanding problems of rational materials design. Emerging applications, such as the high-entropy alloys (HEAs) [1], pose new challenges to computational materials methods. HEAs are defined as alloys with five or more constituent elements in equal or close to equal proportions [1]. A large number of elements leads to high configuration entropy of the solid solution phase and hence stabilizes it. Owing to this, HEAs possess many unique mechanical properties [2–4]. Accurate computational prediction of the mixing enthalpy and configuration entropy would be very instrumental in studying HEAs, as it is hard to experimentally explore different compositions of five or more elements due to combinatorial complexity. The state-of-the-art methodology of computationally assessing the stability of multicomponent crystalline alloys is based on cluster expansion [5, 6], allowing to fit formation energies of binary systems over the entire range of compositions, and ternary and quaternary systems [7–10] over, typically, some subrange of the composition range.

In this Letter I propose a new approach to accurately representing and fitting the formation energies of alloys with a large number of elements with an error of 2 to 6 meV/atom over the entire range of compositions. The approach is based on partitioning the energy into contributions of the atomic environments and representing these contributions with low-rank multidimensional tensors [11]. The proposed model has only two adjustable parameters, the range of the interatomic interaction and the upper bound on the tensor rank, the latter controls the number of free parameters in the model. The idea of a low-rank representation of functions of the atomic environments was also pursued in [12].

I consider the following on-lattice model of a crystal. Let the positions of atoms be  $A\mathbb{Z}^3$ , where  $\mathbb{Z}^3$  is the lattice of all points with integer coordinates and the matrix  $A$  sets the actual crystal structure and dimensions. For example, a face-centered cubic (f.c.c.) lattice with constant  $a$  is defined by  $A = \begin{pmatrix} 0 & a/2 & a/2 \\ a/2 & 0 & a/2 \\ a/2 & a/2 & 0 \end{pmatrix}$ . Each atom  $\xi \in A\mathbb{Z}^3$  is of the type  $x(\xi) \in \{1, \dots, m\}$  [13]. Let  $\Omega \subset A\mathbb{Z}^3$

be a computational domain (supercell) repeated periodically in the entire space. Then the degrees of freedom of the atomistic system are  $x(\xi)$  for all  $\xi \in \Omega$ . The atoms are assumed to interact only with their closest environment characterized by the cut-off distance  $R_{\text{cut}}$  and the interaction neighborhood comprised of all vectors  $r_1, \dots, r_n \in A\mathbb{Z}^3$  whose length is less than  $R_{\text{cut}}$ . Hence, the energy of interaction of these atoms is postulated to be

$$E(x) = \sum_{\xi \in \Omega} V(x(\xi + r_1), \dots, x(\xi + r_n)), \quad (1)$$

where  $V$  is the interatomic potential. Essentially,  $V$  is an  $m \times m \times \dots \times m$ ,  $n$ -dimensional tensor that defines the interaction model (1). The goal is to fit this model to the “true” quantum-mechanical model given by  $E^q(x)$ . Without loss of generality it can be assumed that  $E^q(x) = 0$  whenever all  $x(\xi)$  are equal—in this case  $E^q(x)$  is called the formation energy of  $x$ . The fitting is done on a set of  $K$  atomistic configurations  $x^{(k)}$ ,  $k = 1, \dots, K$ , given together with their true energies  $E^q(x^{(k)})$ . Then, the sought  $V$  is obtained by minimizing the mean-square functional

$$\frac{1}{K} \sum_{k=1}^K \left| E(x^{(k)}) - E^q(x^{(k)}) \right|^2. \quad (2)$$

This is a linear regression problem on the multidimensional tensor  $V$ .

The typical datasets quoted in the literature have a few thousands of configurations, whereas, for example, for an f.c.c. crystal even for two species ( $m = 2$ ) and 12 nearest neighbors ( $n = 13$ ) we have  $m^n = 8192$  unknown parameters fitting which already seems intractable. Accounting, however, for physical symmetries (i.e., enforcing  $V$  to be invariant with respect to the f.c.c. crystal symmetry space group) reduces the number of unknowns to 288 and the problem becomes tractable. However, if the number of species increases to  $m = 3$  then the number of unknowns becomes of the order of  $10^5$  which could still be handled with the compressive sensing, but for  $m > 4$  a different way of reducing the number of unknowns needs

to be applied. Below I show that the so-called low-rank tensor representation for  $V$  successfully reduces the number of unknowns in the regression problem and yields an efficient way of accurately fitting the formation energies.

Next, I review the concept of low-rank tensors. Consider an  $m \times m$  matrix  $M = M(i, j)$ , where  $i, j \in \{1, \dots, m\}$ . The matrix has rank  $r$  or less if it can be represented as

$$M(i, j) = \sum_{\ell=1}^r u_{\ell}(i) v_{\ell}(j),$$

where  $u$  and  $v$  are the scaled singular vectors of  $M$ . As a natural generalization, we can say that a tensor  $V$  has rank  $r$  if

$$V(x_1, \dots, x_n) = \sum_{\ell=1}^r u_{\ell}^{(1)}(x_1) \dots u_{\ell}^{(n)}(x_n) \quad (3)$$

for some  $u_{\ell}^{(1)}, \dots, u_{\ell}^{(n)}$ . It is known that the set of tensors of the form (3) is not a closed set (and therefore might not behave well in optimization problems). This can be illustrated, for example, by taking a simple one-body energy  $V(x_1, \dots, x_n) = \varphi(x_1) + \dots + \varphi(x_n)$  which is a rank- $n$  tensor, but it can be approximated with an arbitrary accuracy by the following rank-two tensor:

$$\frac{(1 + \epsilon \varphi(x_1)) \dots (1 + \epsilon \varphi(x_n)) - 1}{\epsilon} \approx (\varphi(x_1) + \dots + \varphi(x_n)).$$

I will therefore use the Tensor Train (TT) representation which is known to be free from this problem:

$$V(x_1, \dots, x_n) = A^{(1)}(x_1) \dots A^{(n)}(x_n), \quad (4)$$

where  $A^{(i)}(x_1)$  is an  $x_1$ -dependent matrix of size  $r_{i-1} \times r_i$ , and  $r_0 = r_n = 1$ . The matrices  $A^{(i)}$  are called the cores of the TT representation. The rank of this representation is defined as  $\bar{r} := \max_i r_i$ .

I thus assume that the interatomic potential  $V$  has the form (4), where, after  $R_{\text{cut}}$  is fixed,  $\bar{r}$  is the only parameter controlling the accuracy of the model. The  $x$ -dependent matrices  $A^{(i)}$  are the unknown parameters of the model that are found by fitting to the ab initio data. It should be noted that (4) is not invariant with respect to the space group of the cubic lattice,  $G$ , consisting of 48 linear space transformations  $g \in \mathbb{R}^{3 \times 3}$  that map  $\mathbb{A}\mathbb{Z}^3$  into itself. The mean-square functional (2) is therefore adjusted to

$$J := \frac{1}{48K} \sum_{g \in G} \sum_{k=1}^K \left| E(g(x^{(k)})) - E^q(x^{(k)}) \right|^2. \quad (5)$$

The training (fitting) problem is hence:

find  $A^{(1)}, \dots, A^{(n)}$  minimizing  $J$  subject to (1) and (4).

To solve this optimization problem, it should be noted that the functional  $J$  is quadratic in  $E$ , the latter is linear in  $V$ , and  $V$  is a multilinear function of  $A^{(1)}, \dots, A^{(n)}$ . I hence use the alternating least squares (ALS) algorithm, consisting of taking an initial guess for all  $A^{(i)}$  and then updating  $A^{(i)}$  in an iterative manner until convergence. Each iteration consists of  $n$  subiterations, in the  $i$ -th subiteration  $J$  is minimized with respect to  $A^{(i)}$  while freezing other  $A^{(j)}$ ,  $j \neq i$ . The latter is a standard quadratic optimization problem which is equivalent to solving a system of linear algebraic equations and is solved by the Gauss–Seidel method. As a final component of the algorithm, the simulated annealing is used in order to avoid the iterations getting stuck in local minima.

The iterations are stopped when the difference in  $J$  between two consecutive iterations is less than a certain threshold. The value  $\sqrt{J}$  then is the training root-mean-square error (RMSE). In case if the training set size,  $K$ , is small, it can be significantly smaller than the actual prediction (validation) error of the model. To assess the latter, a validation set  $\tilde{x}^{(1)}, \dots, \tilde{x}^{(\tilde{K})}$  is generated independently of the training set and the validation RMSE is then  $\tilde{J}^{1/2}$ , where

$$\tilde{J} := \frac{1}{48\tilde{K}} \sum_{g \in G} \sum_{k=1}^{\tilde{K}} \left| E(g(\tilde{x}^{(k)})) - E^q(\tilde{x}^{(k)}) \right|^2.$$

In what follows, by the fitting error I mean the validation RMSE.

To test the proposed fitting method, I calculate and fit the formation energies of a number of systems using the density functional theory (DFT) as implemented in the VASP package [14, 15], the projected augmented wave (PAW) pseudopotentials [16], and the Perdew–Burke–Ernzerhof exchange-correlation functional [17]. In some tests the atomistic configurations were relaxed: the system was driven to a local minimum with respect to the atomic positions and the supercell size and shape. Unless stated otherwise, the atomistic configurations were generated as follows. The computational cell was a cube with the side of 8 Å containing 32 atoms arranged in an f.c.c. lattice with the lattice constant of 4 Å. The  $\Gamma$ -centered  $4 \times 4 \times 4$  k-point mesh was used. This ensures that the DFT energies are converged to about 1.3 meV/atom accuracy. The configurations with  $m$  species were generated randomly and independently from each other, by first uniformly sampling  $m$  numbers,  $n_1, \dots, n_m$  such that  $n_1 + \dots + n_m = 32$ , and then for each species  $i$ ,  $n_i$  atoms of that species are placed in the free sites of the lattice. This ensures that the entire range of alloy compositions is properly covered.

For each test the two sets of configurations were generated: the training set of varying size which was used for the fitting and the validation set of 200 to 400 configurations that were not involved in the fitting and on which

the (prediction) error was measured. The fitting was then done with a sequence of  $\bar{r} = 2, 3, \dots$ , and the value of  $\bar{r}$  for which the 10-fold cross-validation error [18] was minimal was chosen. Cross-validation is a technique of estimating the validation error based only on the training set. Unless stated otherwise, the 13-atom nearest-neighbor model was used.

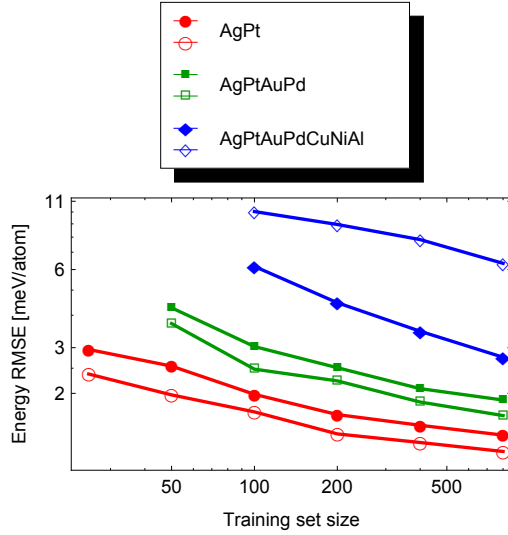


FIG. 1. The learning curves (i.e., the root-mean-square energy error as measured on the validation set as a function of the training set size) for three different systems. The filled markers correspond to the fitting of unrelaxed configurations, while the hollow markers correspond to the fitting of relaxed ones.

The first test demonstrates an excellent performance of the proposed fitting method on a sequence of three systems, Ag-Pt, Ag-Pt-Au-Pd, and Ag-Pt-Au-Pd-Cu-Ni-Al. The results of this test are shown in Fig. 1. When fitting the formation energy of the unrelaxed configurations, the training set size of approximately 25, 100, or 600 configurations was sufficient to reach the accuracy of 3 meV/atom for, respectively, the binary, quaternary, and septenary systems. When fitting the energy of the relaxed Ag-Pt or Ag-Pt-Au-Pd configurations, the error was even smaller than that for the unrelaxed configurations. In contrast, the fitting error of the relaxed septenary alloy configurations was about twice larger than that of the relaxed configurations. The latter may be attributed to large relaxations in the Ag-Pt-Au-Pd-Cu-Ni-Al system due to significantly different sizes of atoms, which a displacement-free model cannot capture. The following tests are intended to study the approximation properties of the proposed fitting method and therefore were all done on the unrelaxed configurations.

In the next test we will see that the fitting error shows stronger dependence on the number of groups (i.e., periodic table columns) that the alloy elements belong to,

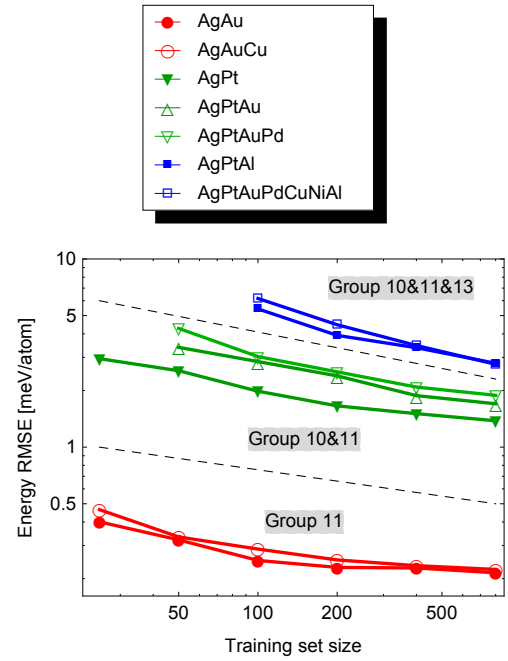


FIG. 2. The learning curves for seven different systems. The error depends strongly on the number of groups that the elements belong to.

and weaker dependence on the number of elements themselves. As can be seen from Fig. 2, the fitting error of the ternary system of group 11 elements is smaller than that of the Ag-Pt system, and the error of the quaternary system with groups 10 and 11 elements is smaller than that of the Ag-Pt-Al system. The latter error is essentially the same as for the septenary system with elements from the three groups. Another remarkable property that can be seen in Fig. 2 is that the errors for the systems with elements from the same group is an order of magnitude smaller than that for the other systems.

The results shown in Fig. 2 naturally raise the following question: can the systems with elements from two or more groups be fitted with the accuracy lower than 1 meV/atom by refining the  $k$ -points mesh and possibly modifying the fitting scheme? The results below suggest that it is not possible without vastly increasing  $R_{\text{cut}}$  (and therefore the training set size).

Four different fits were obtained for the Ag-Pt system: two models, the one with  $n = 13$  (first-nearest-neighbor model) and the other one with  $n = 19$  (next-nearest-neighbor model), were fitted to two sets of QM data, the one with  $4 \times 4 \times 4$   $k$ -point mesh ( $k$ -point spacing of  $0.031\text{\AA}^{-1}$ ) and the other with  $8 \times 8 \times 8$   $k$ -point mesh ( $k$ -point spacing of  $0.016\text{\AA}^{-1}$ ). The latter  $k$ -point mesh ensures that the DFT energies are converged to the accuracy of about 0.1 meV/atom. The corresponding learning curves (i.e., the error as a function of the training set size

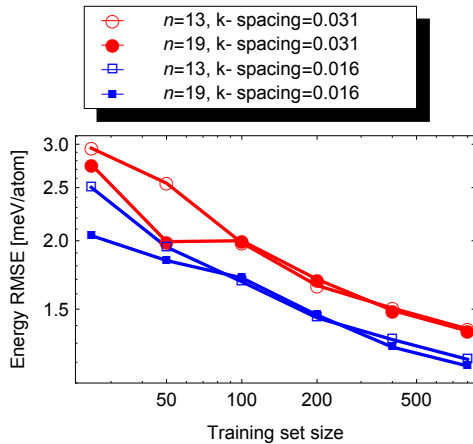


FIG. 3. Learning curves for different interaction ranges ( $n = 13$  and  $n = 19$ ) and different DFT accuracies (k-point spacing of  $0.031\text{\AA}^{-1}$  and  $0.016\text{\AA}^{-1}$ ). The graphs indicate that the error cannot be reduced further without increasing the interaction range.

$K$ ) are shown in Fig. 3. These results indicate that including the next nearest neighbors does not significantly improve the results, and fitting to highly converged DFT energies improves the error only slightly, by about 10%.

Finally, the nearest-neighbor model fitted without the low-rank restriction on 800 Ag-Pt configurations was compared to the low-rank fit. Without the low-rank restriction the model has 288 coefficients that were fitted to 800 energies. The validation error of this model was 2.15 meV/atom and the fitting error was 1.0 meV/atom. This indicates that lifting the low-rank restriction cannot significantly improve the error.

The results above confirm that a large part of the remaining 1–3 meV/atom errors shown in Fig. 1 is due to nonlocality in the interatomic interaction. This nonlocality can be explained by the fact that the electron density perturbation in metals decays slowly [19]. This means that replacing an atom in a configuration by another atom with a different number of valence electrons creates a nonlocal perturbation, whereas replacing atoms while keeping the same number of valence electrons introduces a more local perturbation. This is in agreement with the fact that the Ag-Au and Ag-Au-Cu systems could be fitted much more accurately compared to the other systems.

In conclusion, the low-rank approximation of the interatomic interaction tensor demonstrates excellent performance in the fitting of multicomponent alloys unattainable, presently, by the cluster expansion method. The proposed fitting method is simple and has only two adjustable parameters—one to control the range of the interaction and the other one to control the number of fitting parameters. The fitting procedure needs nonlinear

optimization, however, the evaluation of the fitted model is very fast: it reduces to performing, for each atom, a few multiplications of a small matrix by a vector. I expect that this method will be useful in directly computing the mixing enthalpy and configuration entropy of alloys with many components.

The author thanks Prof. Jörg Neugebauer, Prof. Gábor Csányi and Prof. Alexandre Tkatchenko for valuable discussions. This work was supported by the Skoltech NGP Program No. 2016-7/NGP (a Skoltech-MIT joint project). A part of the work was done by the author during the Fall 2016 long program at the Institute of Pure and Applied Mathematics, UCLA.

---

- [1] J.-W. Yeh, S.-K. Chen, S.-J. Lin, J.-Y. Gan, T.-S. Chin, T.-T. Shun, C.-H. Tsau, and S.-Y. Chang, *Advanced Engineering Materials* **6**, 299 (2004).
- [2] Y. Zhang, T. T. Zuo, Z. Tang, M. C. Gao, K. A. Dahmen, P. K. Liaw, and Z. P. Lu, *Progress in Materials Science* **61**, 1 (2014).
- [3] B. Gludovatz, A. Hohenwarter, D. Catoor, E. H. Chang, E. P. George, and R. O. Ritchie, *Science* **345**, 1153 (2014).
- [4] O. Senkov, G. Wilks, D. Miracle, C. Chuang, and P. Liaw, *Intermetallics* **18**, 1758 (2010).
- [5] L. J. Nelson, G. L. Hart, F. Zhou, V. Ozoliņš, *et al.*, *Physical Review B* **87**, 035125 (2013).
- [6] Q. Wu, B. He, T. Song, J. Gao, and S. Shi, *Computational Materials Science* **125**, 243 (2016).
- [7] Y. Zhang, V. Ozolins, D. Morelli, and C. Wolverton, *Chemistry of Materials* **26**, 3427 (2014).
- [8] J. S. Wróbel, D. Nguyen-Manh, M. Y. Lavrentiev, M. Muzyk, and S. L. Dudarev, *Physical Review B* **91**, 024108 (2015).
- [9] S. Hao, L.-D. Zhao, C.-Q. Chen, V. P. Dravid, M. G. Kanatzidis, and C. M. Wolverton, *Journal of the American Chemical Society* **136**, 1628 (2014).
- [10] S. Maisel, M. Höfler, and S. Müller, *Physical Review B* **94**, 014116 (2016).
- [11] I. V. Oseledets, *SIAM Journal on Scientific Computing* **33**, 2295 (2011).
- [12] M. d’Avezac, R. Botts, M. J. Mohlenkamp, and A. Zunger, *SIAM Journal on Scientific Computing* **33**, 3381 (2011).
- [13] In the cluster expansion literature the degrees of freedom are typically denoted by  $\sigma(\xi)$ , following the notation of the electron spin.
- [14] G. Kresse and J. Hafner, *Physical Review B* **47**, 558 (1993).
- [15] G. Kresse and J. Furthmüller, *Physical review B* **54**, 11169 (1996).
- [16] P. E. Blöchl, *Physical Review B* **50**, 17953 (1994).
- [17] J. P. Perdew, K. Burke, and M. Ernzerhof, *Physical review letters* **77**, 3865 (1996).
- [18] E. Alpaydin, *Introduction to machine learning* (MIT press, 2014).
- [19] A. Gabovich, L. Il’Chenko, E. Pashitskii, and Y. A. Romanov, *Soviet Journal of Experimental and Theoretical Physics* **48**, 124 (1978).